11-1-2002

Sustained Potential Oscillations in Proton Exchange Membrane Fuel Cells with PtRu as Anode Catalyst

J. X. Zhang

Ravindra Datta
Worcester Polytechnic Institute, rdatta@wpi.edu

Journal of The Electrochemical Society, **149** (11) A1423-A1431 (2002)
0013-4651/2002/149(11)/A1423/9/$7.00 © The Electrochemical Society, Inc.

Sustained Potential Oscillations in Proton Exchange Membrane Fuel Cells with PtRu as Anode Catalyst

Jingxin Zhang* and Ravindra Datta,z**

Fuel Cell Center, Department of Chemical Engineering, Worcester Polytechnic Institute, Worcester, Massachusetts 01609, USA

Sustained potential oscillations are experimentally observed in a proton exchange membrane fuel cell with PtRu as anode catalyst and with H_2/108 ppm CO as the anode feed when operating under a constant current density mode. These oscillations appear at fuel-cell temperatures below 70°C. A threshold value exists for both the current density and the anode flow rate at a given fuel-cell temperature for their onset. The temperature dependence of the oscillation period shows an apparent activation energy around 60 kJ/mol. The potential oscillations are believed to be due to the coupling of anode electro-oxidation of H_2 and CO on the PtRu catalyst surface, on which OH_{ad} is formed more readily, *i.e.*, at lower overpotentials. A simple kinetic model is provided that can reproduce the observed oscillatory phenomenon both qualitatively and quantitatively.
 [DOI: 10.1149/1.1511752]

Manuscript submitted February 11, 2002; revised manuscript received May 6, 2002. Available electronically September 26, 2002.

The proton exchange membrane (PEM) fuel cell is emerging as a promising power source for both vehicular and stationary applications.[1] However, due to the difficulties associated with hydrogen storage and distribution, liquid fuels such as methanol and gasoline are planned to be processed on demand for generation of a hydrogen-rich gas as feed to PEM fuel-cell anodes. Such a feed stream will inevitably contain trace amounts of CO. Since the conventional Pt anode electrocatalysts are rendered ineffective with feeds containing even 5-10 ppm CO, PtRu anode catalysts have been developed that provide increased tolerance to CO poisoning. In our effort to investigate the performance and H_2/CO electro-oxidation mechanism on PtRu electrocatalysts, we found sustained potential oscillations in a PEM fuel cell operated under constant current density with a H_2/CO anode feed under practically relevant conditions.

Oscillatory phenomena are not uncommon in electrochemical systems.[2] Metal dissolution and deposition is reported to give potential oscillations in alkaline solutions.[3-6] It is also found that galvanostatic potential oscillations appear when some small organic molecules such as formic acid and formaldehyde are electro-oxidized at the anode.[7-13] Okamoto *et al.* have reported the potential oscillations during the electro-oxidation of formaldehyde in aqueous H_2SO_4 electrolyte.[7-9] Techniques such as electrochemical quartz crystal microbalance (EQCM)[10-11] and probe beam deflection (PBD)[12] have been used to follow the changes occurring on the electrode surface and the electrode/electrolyte interface during the potential oscillations in anodic oxidation of formic acid. Potential oscillations are also found in connection with the anodic oxidation of H_2 on platinum electrodes when metal cations such as Cd^{2+}, Cu^{2+}, Sn^{2+}, Bi^{3+}, and Ag^{+} are present in the electrolyte solution.[14-16] These oscillations are believed to be due to the coupling of hydrogen oxidation and the electrosorption and/or electrodeposition and dissolution of the metal ions. A similar coupling effect was also observed when H_2 containing low concentrations of CO was oxidized on Pt electrodes in an electrochemical cell with liquid electrolyte, resulting in potential oscillations at constant current density.[17-19] These oscillations were ascribed to a passivation-type polarization curve in the electrode reaction.[19]

There are many reports in the literature on the modeling of oscillatory processes in electrochemical systems. Thus, Wolf *et al.*[20] provide a model for the galvanostatic oscillations that occur during the oxidation of hydrogen at a platinum electrode in the presence of electrosorbing metal ions and specifically adsorbing anion. The temporal change in the potential at the electrode was deduced by considering the total current density as a sum of the capacitive and charge-transfer current densities, the latter comprising the charge passed during the oxidation of the hydrogen and the adsorption and desorption of the metal ions. Okamoto *et al.*[21] provide a model to reproduce the observed kinetic potential oscillations for the electrochemical oxidation of formic acid on Pt based on the assumptions that the water adsorption velocity is proportional to the surface coverage of CO, and that the saturation coverage of adsorbed CO is less than 1. Another assumption is that both the forward and backward step of water adsorption depends upon potential, although it is considered a nonelectrochemical step. Yamazaki and Kodera[17] provide a model for hydrogen oxidation in H_2SO_4 solutions in the presence of metal ions such as silver, gold, or gas impurities such as CO. A specific assumption in their model is that attractive interaction exists among CO_{ad}, which is necessary for the appearance of oscillation by the model. Detailed experimental and modeling work was reported by Strasser *et al.*[22] on the current oscillations during electro-oxidation of formic acid on Pt under potentiostatic control. In this work, the scanned current/potential behavior as well as current oscillations were simulated successfully. Their model takes into account two possible reaction pathways for formic acid electro-oxidation and provides bifurcation analysis and mechanistic categorization of the oscillators.

Thus, although many reports exist on oscillatory phenomena in the electrochemical cell system, there is no systematic report on potential oscillations in PEM fuel cells so far in the literature. As far as we know, there is only one recent report that briefly mentions oscillations in a study of PEM fuel-cell performance with feed containing CO.[23] This paper reports for the first time, a systematic study of potential oscillations in a PEM fuel cell with PtRu as the anode catalyst. Sustained potential oscillations were observed when the fuel cell was operated at a constant current density with a H_2/CO anode feed under practically relevant fuel-cell conditions. Experimental conditions that lead to such potential oscillations are presented here. Further, a realistic theoretical model is described based on a kinetic analysis of the reaction on a PEM fuel-cell anode in the presence of CO. This model uses few assumptions to satisfactorily reproduce the oscillatory pattern observed in the experimental work.

Experimental

Gas diffusion electrodes with 20 wt % Pt/C or PtRu/C catalyst were purchased from E-TEK, Inc. (Somerset, NJ). A Pt electrode with a metal loading of 0.4 mg/cm^2 was used as the cathode. A PtRu (atomic ratio 1:1) electrode with a metal loading of 0.35 mg/cm^2 was used as the anode. Nafion® 115 proton exchange membrane (DuPont, Fayetteville, PA) was used after sequential treatment with 2% H_2O_2, deionized water, 0.5 M H_2SO_4, and again with deionized water in order to remove any inorganic and organic impurities. The

* Electrochemical Society Student Member.
** Electrochemical Society Active Member.
z E-mail: rdatta@wpi.edu

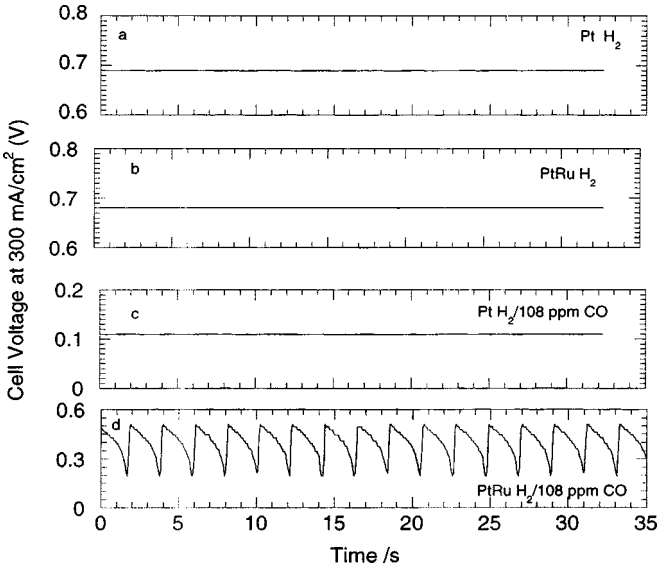

Figure 1. Fuel-cell voltage pattern for (a) Pt with H_2, (b) PtRu with H_2, (c) Pt with H_2/108 ppm CO, and (d) PtRu with H_2/108 ppm CO. Other operation conditions are identical: cell temperature 42°C; current density 300 mA/cm^2; anode inlet flow rate 36.4 sccm.

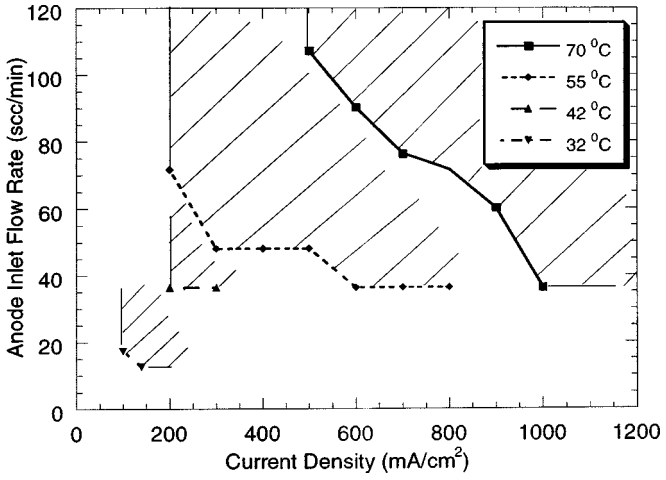

Figure 2. The current density-anode flow rate domain where anode overpotential oscillation appears at different temperatures.

membrane electrode assembly (MEA) was prepared by hot-pressing in a model C Carver hot press at 130°C and under a pressure of 4000 lb for about 2 min. The MEA was then assembled in a 5 cm^2 single cell from ElectroChem, Inc. (Woburn, MA), and tested in a test station with temperature, pressure, humidity, and flow rate control. The fuel-cell voltage was recorded using an HP 6060B dc electronic load, interfaced with a PC using LabVIEW software (National Instruments, Austin, TX) at a data sampling rate of 77 ms.

The single PEM fuel cell thus assembled was tested at different temperatures. Anode and cathode gases were first humidified through a stainless steel bottle containing water at the desired temperature before being fed into the fuel cell. The temperature of the humidification bottle was set at 15 and 10°C higher than that of the fuel cell for the anode and cathode side, respectively, accounting for the heat losses and resulting condensations between the humidifier and the fuel cell. The total pressure of both the anode and the cathode was 30 psig unless otherwise indicated. The flow rates reported in this study are in units of standard (1 atm and 25°C) cubic centimeter per minute (sccm). Premixed H_2/108 ppm CO was purchased from MG Industries (Morrisville, PA) and was used as the anode feed. The CO concentration was certified by the supplier and was not independently confirmed. Oxygen was used as the cathode feed.

Results

Onset of potential oscillations.—The single PEM fuel cell was tested with pure hydrogen as well as H_2/108 ppm CO using Pt and PtRu as anode catalyst, respectively. The results are shown in Fig. 1. The cell voltage is plotted *vs.* time for the single cell operated under identical conditions (fuel-cell temperature 42°C, current density 300 mA/cm^2, anode flow rate 36.4 sccm) except for those indicated inside the figure. It was found, as expected, that the cell voltage remained steady when pure hydrogen was used as the fuel for both Pt and PtRu anode catalysts. When the fuel was switched over to H_2/108 ppm CO, periodic voltage oscillations appeared for the fuel cell with PtRu anode catalyst but not for Pt. Such comparisons were conducted at all other experimental conditions where sustained potential oscillations were observed for the case of the H_2/CO and PtRu system. Based on these results, it is clear that the observed oscillations are unique to the H_2/CO feed and the PtRu anode in a PEM fuel cell under the conditions investigated.

The voltage oscillations appear only under certain operation conditions. It was observed that proper combination of fuel-cell temperature, current density, and anode flow rate are crucial for the onset of the limit cycle. It was found that temperature is the most critical factor in determining the occurrence of voltage oscillations. No oscillations were observed when the cell temperature was above 80°C, but they occurred commonly below 70°C. Further, for a given temperature, potential oscillations were found to exist only in a certain range of current density and anode flow rate. Figure 2 shows roughly the current density-anode flow rate domains at different fuel-cell temperatures where the potential oscillations appear. The domain becomes smaller at lower temperatures since only small current densities can be sustained at lower temperatures in the PtRu anode PEM fuel cell with a H_2/CO feed. It is evident that the domain boundary in Fig. 2 should be smooth, but unfortunately, the experiments can only be performed in a discrete manner. It is a common observation that chemical oscillations typically appear only in a very narrow range of parameter values that are deducible, in principle, from the mathematical relations governing the dynamic system.[24]

It is seen that the current density must be larger than a limiting value at a given anode flow rate, and vice versa, for the voltage oscillations to appear. The existence of a threshold current for the onset of potential oscillation has been reported in other works, such as in H_2 electro-oxidation in the presence of metal cations (about 70 μA for a 20 cm^2 Pt wire)[16] or low concentration of CO in a liquid electrolyte (75 mA/cm^2 for a platinized porous carbon electrode).[19]

The transition between steady conditions and a limit cycle with anode flow rate change is shown in Fig. 3. Thus, when the anode flow rate is increased from 48.1 to 60.1 sccm, sustained voltage oscillations appear. When the anode flow rate is changed back to the original lower flow rate, the voltage oscillations become dampened and eventually disappear. The transition of cell voltage from a steady value to a periodic oscillation was also observed when the current was crossed over from a value in the nonoscillating domain to one which leads to oscillations at a given flow rate.

Effect of current density.—The cell voltage oscillations are clearly caused by periodicity in the anode overpotential. In order to single out the anode overpotential, the cell voltage for the case of pure H_2 was also measured at otherwise identical experimental conditions. The overall fuel-cell voltage is[25,26]

$$V = V_0 - \eta_A + \eta_C - i\left(\frac{L}{\sigma}\right) - i(R_I) \qquad [1]$$

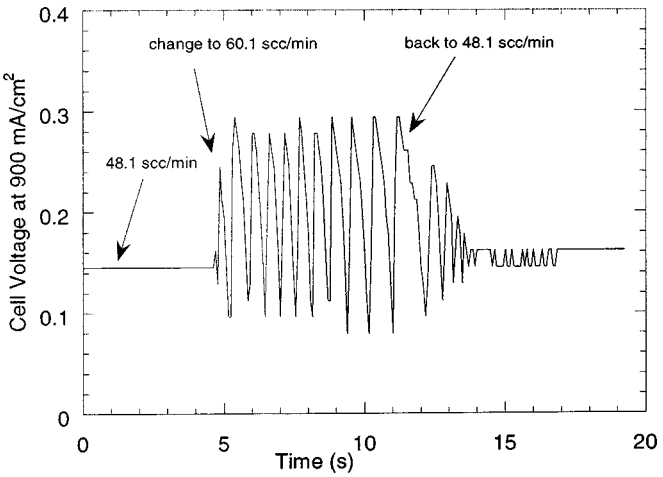

Figure 3. The transition of the fuel-cell voltage between a steady value and oscillation with the variation of anode flow rate. Cell temperature 70°C; current density 900 mA/cm^2.

where V_0 is the open-circuit potential, i is the current density, η_A and η_C are the anode and cathode overpotentials, including any diffusional overpotential in the gas-diffusion layer, respectively, L and σ are the thickness and conductivity of the PEM, respectively, while R_I is any interfacial resistance. Thus, at a constant current density, the difference in the polarization of the anode between the cases of the presence ($\eta_{H_2/CO}$) and the absence of CO (η_{H_2}) in anode feed may be obtained simply from the corresponding measurements of the cell voltage

$$\eta_{H_2/CO} - \eta_{H_2} = V_{H_2} - V_{H_2/CO} \quad [2]$$

where V_{H_2} and $V_{H_2/CO}$ are the cell voltages with H_2 and H_2/CO feed, respectively. Further, since the overpotential for pure H_2 is small, it may be neglected without substantial error. Thus, the anode overpotential in the presence of CO is assumed to be simply the cell voltage difference between the two cases, *i.e.*

$$\eta_{H_2/CO} \approx V_{H_2} - V_{H_2/CO} \quad [3]$$

Figure 4 shows a series of thus-obtained anode overpotential oscillatory patterns at 55°C and various current densities, while the anode flow rate was kept at a constant value of 48.1 sccm. It is seen that the pattern of these oscillations is largely unaffected as the current density is increased from 300 to 700 mA/cm^2. One noteworthy feature of the oscillations at different current densities is that the minimum overpotential appears to be more uniform than the maximum. Further, the maximum and minimum potentials are not greatly dependent upon the current density, except for the fact that the amplitude of overpotential oscillations at 300 mA/cm^2 is about 50-60 mV lower than that at other current densities. The oscillation period of about 0.9 s also does not change very much with the applied current density. In the study of potential oscillations in H_2-CO oxidation on Pt electrode in an electrochemical cell, Deibert and Williams[19] found that the oscillation frequency does not change for current density between 200 and 500 mA/cm^2, although they found that the frequency decreases slightly with the increase of current density in the range of 75-200 mA/cm^2. In the study of H_2 electrooxidation in the presence of Cu^{2+} by Krischer *et al.*[16] and formaldehyde oxidation in H_2SO_4 solution by Okamoto *et al.*,[8] an oscillation pattern transition was found with current density and operation time. For example, period-doubling or tripling, or even aperiodicity, was observed accompanying the increase of the current density and the elapse of time. However, such transitions with current density and time were not found in this study.

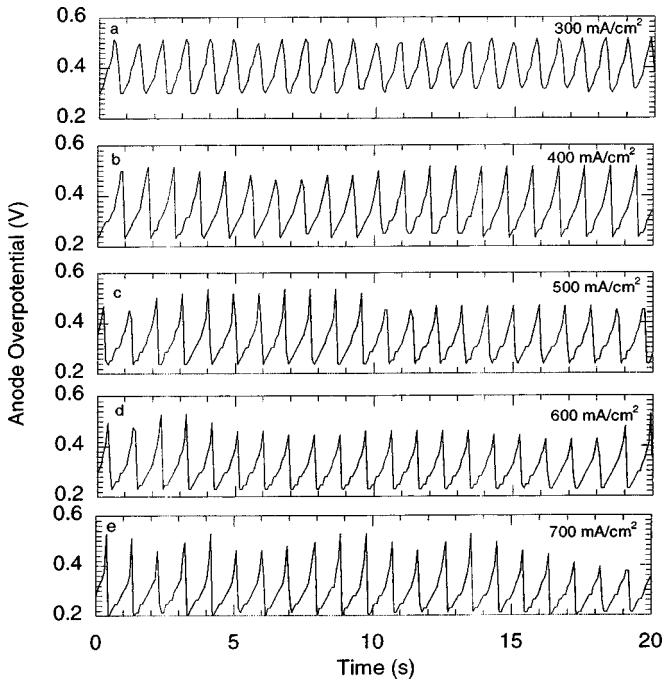

Figure 4. Potential oscillation of PEM fuel cell at 55°C at different current densities: (a) 300, (b) 400, (c) 500, (d) 600, and (e) 700 mA/cm^2. Anode flow rate is 48.1 sccm for all cases.

Effect of anode flow rate.—The anode inlet flow rate is an important parameter for the onset of anode potential oscillations, as illustrated in Fig. 2. Therefore, the effect of anode flow rate on the oscillations was further investigated as shown in Fig. 5, where the anode overpotential is plotted *vs.* time at 42°C and 300 mA/cm^2 for different anode flow rates. Although the general shape and the period of oscillations does not change as the anode flow rate is changed from 36.4 to 71.6 sccm, the amplitude is somewhat affected. This can be seen in Fig. 6, where the maximum overpotential increases while the minimum overpotential decreases with increasing anode inlet flow rate. As discussed in our previous work,[26] the CO concentration in the anode compartment is a function of anode flow rate and thus, the anode overpotential increases with anode flow rate. Therefore, the observed effect is likely due to the increasing CO concentration in the anode compartment with increasing anode flow rate. Similar trend in the maximum overpotential with the increase of CO bubbling rate was found by Yamazaki *et al.*[15] in

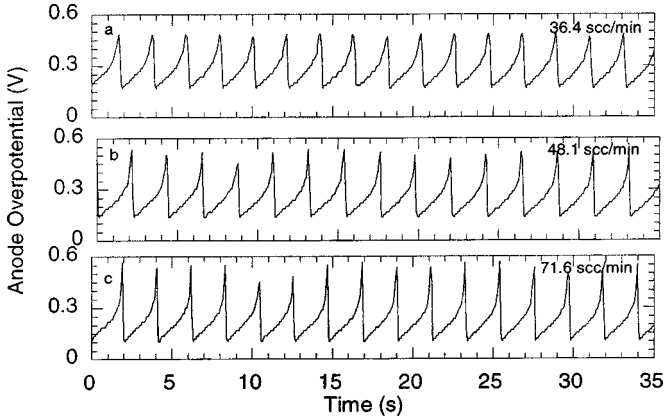

Figure 5. Potential oscillation of PEM fuel cell at 42°C at different anode inlet flow rates: (a) 36.4, (b) 48.1 and (c) 71.6 sccm. The current density is 300 mA/cm^2 for all cases.

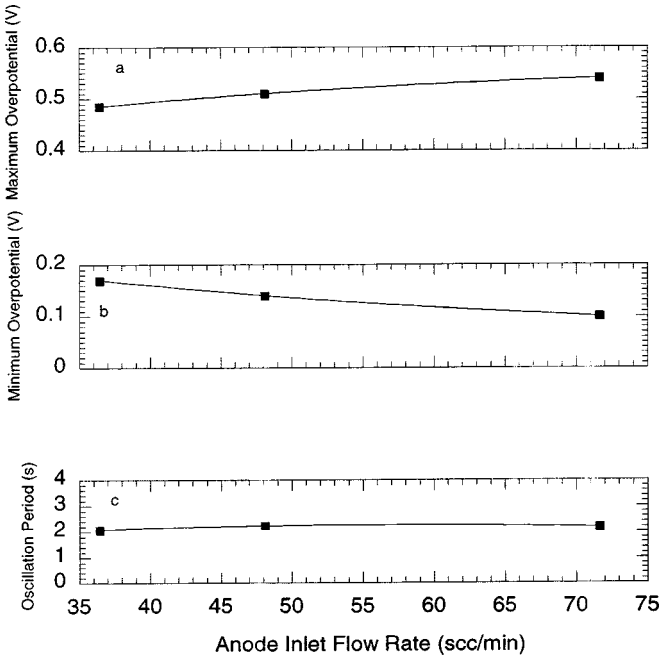

Figure 6. Dependence of (a) maximum and (b) minimum overpotential, (c) oscillation period on anode inlet flow rate for the potential oscillation shown in Fig. 5.

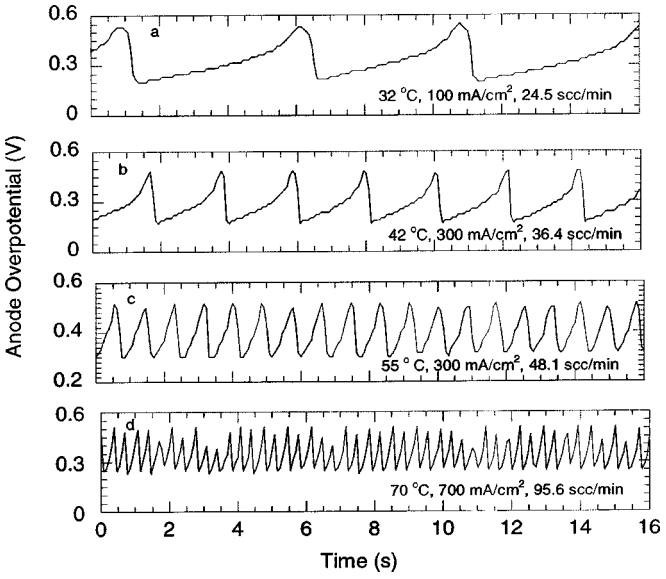

Figure 7. Potential oscillation of PEM fuel cell at different temperatures. The fuel-cell temperature, applied current density, and anode inlet flow rate are, as follows: (a) 32°C, 100 mA/cm^2, 24.5 sccm; (b) 42°C, 300 mA/cm^2, 36.4 sccm; (c) 55°C, 300 mA/cm^2, 48.1 sccm; and (c) 70°C, 700 mA/cm^2, 95.6 sccm.

their study of H_2-CO oxidation on Pt in aqueous electrolyte. Figure 6 also shows that the oscillation period does not change with increasing anode flow rate.

Effect of fuel-cell temperature.—As discussed previously, the oscillation period is relatively insensitive to the anode flow rate and the applied current density in the range investigated. However, it does change dramatically with temperature. Therefore, it is reasonable to compare the oscillation period at different temperatures, even though the corresponding current densities and the anode flow rates are different as a result of the shifting of the limit cycle domain with temperature (Fig. 2).

The oscillatory patterns at four different fuel-cell temperatures are shown in Fig. 7. The shape of anode overpotential change is similar, namely, a gradual increase to the maximum overpotential followed by a rapid drop to the minimum. However, the period decreases dramatically with an increase of fuel-cell temperature, and the potential oscillations disappear altogether at temperatures higher than 70°C. It may be noticed that the oscillation pattern is more pronounced and regular at lower temperatures. The peak value of anode overpotential is below 0.6 V in all cases. This feature may be essential for the occurrence of oscillations in PEM fuel-cell systems. In the literature report of potential oscillations on Pt in the electrochemical cell, the maximum potential is in the range 0.9-1.2 V,[19] which is considerably higher than the cathode potential for appreciable O_2 oxidation current in PEM fuel cells. Actually, the cathode potential is polarized below 0.9 V for a current density of 100 mA/cm^2 at 80°C. Thus, oscillations in a PEM fuel cell with Pt as anode electrocatalyst may not be observed for the H_2/CO feed. The PtRu anode with its lower overpotential for CO electro-oxidation allows such periodic behavior to be observed in a PEM fuel cell.

In order to look more closely at the oscillation process, a magnified picture of the oscillation cycle is shown in Fig. 8a. It can be seen that two branches comprise a cycle. The fast overpotential decline is related to the surface reactivation; the relatively slow ascending branch is a result of the surface CO poisoning and the corresponding electrode polarization. It should be pointed out that the steps in the ascending branch are due to the discrete nature of the reading of the electronic load.

Discussion

The occurrence of the oscillatory behavior is evidently caused by the coupling of the kinetics of electro-oxidation of H_2 and of CO on the anode catalyst. A qualitative explanation is discussed followed by a theoretical model.

With the introduction of CO in the anode feed, the CO begins to build up on the surface until the catalyst surface is almost completely blocked ($\theta_{CO} \rightarrow 1$) due to the strong affinity of CO to the catalyst. In order to sustain the applied current, the anode becomes increasingly polarized to a higher potential. This, in turn, accelerates the electro-oxidation of CO_{ad} on the catalyst surface via the oxygen-containing surface species such as OH_{ad}. At a certain overpotential, the CO electro-oxidation rate exceeds the rate of CO adsorption and

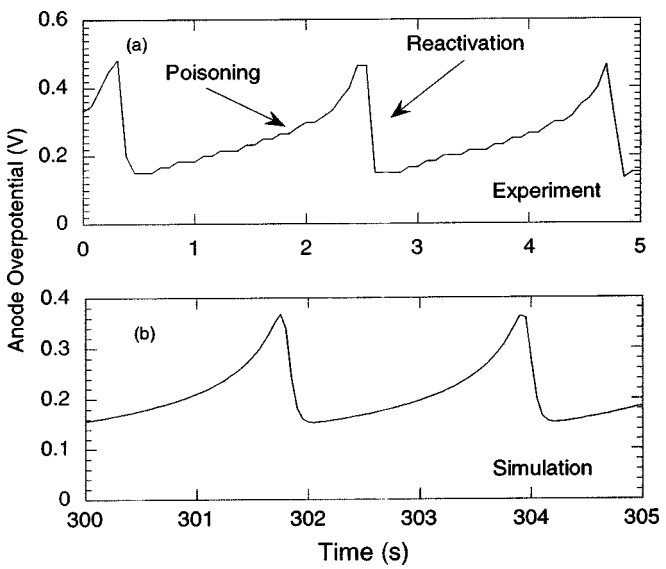

Figure 8. A magnified picture of the potential oscillation pattern from (a) experiment and (b) simulation at 42°C. Current density 300 mA/cm^2; anode inlet flow rate 48.1 sccm.

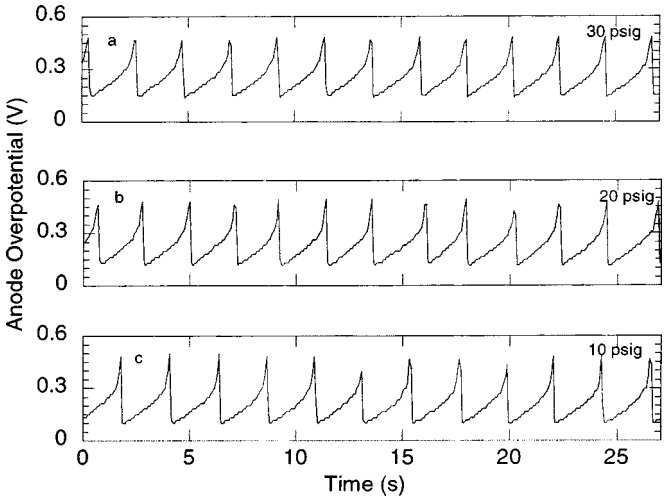

Figure 9. Potential oscillation of PEM fuel cell at 42°C at different cathode O_2 pressures: (a) 30, (b) 20, and (c) 10 psig. Current density 300 mA/cm^2; anode inlet flow rate 48.1 sccm.

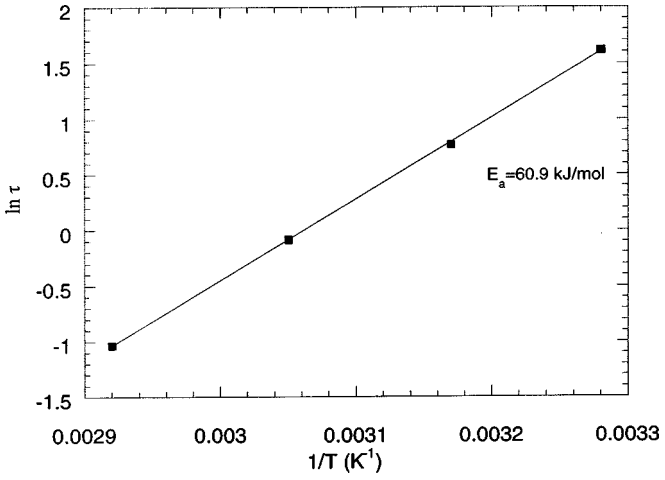

Figure 10. Plot of ln τ *vs.* $1/T$ as per Eq. 5.

the surface coverage of CO declines. At this stage, the H_2 oxidation reaction is no longer limited by the surface coverage of CO, due to the facile kinetics of H_2 electro-oxidation. Thus, the anode overpotential drops quickly to a low value. This potential drop, however, recreates the situation where the rate of CO electro-oxidation is exceeded by that of CO adsorption. Therefore, CO molecules begin to build up again on the catalyst surface and the electrode must again be polarized correspondingly to a higher overpotential. Thus, the cycle is repeated. An explanation of the reason why the potential oscillations do not appear on Pt anode catalysts in PEM fuel cells is that the formation of OH_{ad} species is more facile on Ru surfaces than on Pt surfaces. Thus, Gasteiger *et al.* have shown in their voltammetric study of H_2/CO electro-oxidation that the ignition potential of CO oxidation on Pt is about 0.7-0.9 V[27] at room temperature, when OH_{ad} is appreciably formed on the Pt electrode surface. Even at higher temperatures and lower CO concentrations (*e.g.*, at 60°C and 250 ppm CO), the ignition potential is still above about 0.5 V.[28] The ignition potential of CO oxidation on the PtRu alloy surface is shifted down to 0.3-0.45 V as per the CO stripping voltammetry,[29] since the nucleation of OH_{ad} occurs on PtRu at a lower potential. Therefore, it is likely that in the overpotential range which is available in a PEM fuel cell under normal temperatures, conditions do not exist on Pt where the CO electro-oxidation rate exceeds that of CO adsorption so that periodic cleansing of the surface may be accomplished. However, on the PtRu catalyst, there are periods when H_2 is oxidized on a less contaminated surface temporarily at lower overpotential until CO molecules build up again.

It was found in our previous study[26] that O_2 can also permeate through the PEM from the cathode side to the anode and contribute to the CO oxidation on Pt catalyst via a nonelectrocatalytic direct oxidation pathway. The anode overpotential was thus found to decrease for Pt at higher cathode O_2 pressures. Similar experiments were conducted here to check whether O_2 permeation to the anode has any effect on the oscillatory phenomenon with PtRu catalyst. The oscillation pattern is thus compared for three different cathode O_2 pressures in Fig. 9. It is apparent that the oscillations are not substantially affected as the cathode O_2 pressure is decreased from 30 to 10 psig except for a very small increase in oscillation amplitude. The oscillation period remains essentially constant. In comparison, there is a significant polarization drop of about 0.1 V for the Pt anode catalyst when the cathode pressure is increased from 10 to 30 psig.[26] It thus appears that the direct CO oxidation via a nonelectrocatalytic pathway with oxygen permeating from the cathode on PtRu is less significant as compared with the dominant route via OH_{ad} electro-oxidation. This demonstrates that H_2O is the major agent for CO oxidation on the PtRu catalyst.

As discussed previously, the oscillation period decreases substantially with increasing temperature (Fig. 7). If it is assumed that the oscillation period τ is inversely proportional to the rate constant of a kinetic step, *i.e.*

$$\tau = \frac{C}{A_0 \exp\left(-\frac{E_a}{RT}\right)} \qquad [4]$$

where τ is the oscillation period, C is a constant, A_0 is the preexponential factor, and E_a is the activation energy, then we might expect the following temperature dependence of the oscillation period

$$\ln \tau = \ln\left(\frac{C}{A_0}\right) + \frac{E_a}{RT} \qquad [5]$$

i.e., a plot of $\ln \tau$ *vs.* $1/T$ would yield a straight line with a slope equal to E_a/R. A plot of $\ln \tau$ *vs.* $1/T$ at four different temperatures is shown in Fig. 10. It is seen that a very good linear relationship results with an activation energy of 60.9 kJ/mol. This could serve as a clue in determining which kinetic step might control the frequency of the oscillations.

Possible rate processes controlling the oscillatory behavior include bulk diffusion, adsorption onto the catalyst surface, surface diffusion, and surface reaction of CO and/or H_2. It has been shown by others[30] as well as in our previous work[26] that there are no CO bulk diffusional limitations in fuel-cell anodes for the gas mixture of H_2 containing trace amounts of CO. Further, the adsorption of H_2 and CO on noble metal surfaces is a fast process, with low activation energies. Thus, the limiting process must be either a surface diffusion or a surface reaction step.

A quantitative estimation of the activation energy of the possible surface process was obtained using the unity bond index-quadratic exponential potential (UBI-QEP) method.[31,32] The calculation results together with some experimental data are listed in Table I. It can be seen that the activation energy of the surface reaction between CO_{ad} and OH_{ad}, which is believed to be the elementary step in the electro-oxidation of CO on PtRu surfaces by many researchers, is roughly between 40 and 50 kJ/mol. The dissociation of H_2O on the catalyst surface is an essential step in the formation of OH_{ad}. The activation energy for this step is calculated to be 78.6 kJ/mol on Pt surfaces and 59.8 kJ/mol on Ru. The experimental value for Pt is

Table I. Estimation of the activation energy of some surface steps using the UBI-QEP method.

Surface steps	Activation energy E_a (kJ/mol) UBI-QEP method Pt	Ru	Experimental data Pt
$CO_{ad} + OH_{ad} \rightarrow CO_{2,ad} + H_{ad}$	46.4[a]	46.0[a]	30-40[c]
$H_2O_{ad} \rightarrow OH_{ad} + H_{ad}$	78.6[a]	59.8[a]	105 ± 21[d]
OH_{ad} surface diffusion	23.0[b]	29.5[b]	
CO_{ad} surface diffusion	19[b]	17.3[b]	33.0 ± 8.4[e]

[a] Ref. 31.
[b] Ref. 32.
[c] Ref. 33.
[d] Ref. 34.
[e] Ref. 35.

104.5 ± 20.9 kJ/mol.[34] The theoretical prediction and experimental values of the surface diffusion activation energies are also listed in Table I, and are unlikely to be rate limiting. Therefore, it is plausible that the oscillation is controlled by the surface reaction steps either of OH_{ad} formation or the reaction between OH_{ad} and CO_{ad}. However, due to the uncertainties in calculation of these values, this can not be determined unambiguously.

Modeling

An attempt is made here to simply model the experimentally observed potential oscillations of PEM fuel cells with PtRu as anode catalyst and with H_2/CO as anode feed. The fuel cell is operated in a constant current density mode and the CO concentration is 108 ppm, which is approximately the CO level in the reformate stream after preferential oxidation (PrOx) from a reformer.

The catalyst surface is assumed to be uniform in this model, with the surface site represented by S, *i.e.*, we do not consider a heterogeneous surface with two different metal sites, despite the fact that H_2 is likely to adsorb and dissociate on Pt preferentially, while H_2O is likely to adsorb and dissociate on Ru preferentially. However, in this model, the above-mentioned difference in surface sites is neglected, assuming that alloying alters the energetics and kinetics of the surface reactions. It is also assumed that there is no interaction among surface species, which only interact indirectly via competition for the free surface sites.

At the reactor scale, the fuel-cell temperature is at a fixed value so that isothermal conditions are assumed. The feed stream is always assumed to be saturated with water vapor. The anode chamber is assumed to be well mixed, which is not an unreasonable assumption for a differential or small (5 cm^2) single cell.[26]

The parameters used here are taken from the literature, with the exception of those not available, which were fitted to reproduce the experimental data. There are only two parameters that are fitted, as listed in Table II. The resulting model presented here is able to adequately explain the potential oscillation found in the electro-oxidation of H_2/CO on the PtRu anode catalyst in PEM fuel cells.

Surface chemistry.—The Tafel-Volmer mechanism is assumed for H_2 electro-oxidation, *i.e.*, H_2 is dissociatively chemisorbed on surface sites represented by S, followed by the electrochemical oxidation of adsorbed hydrogen atoms

$$H_2 + 2S \leftrightarrows 2S{-}H \quad \vec{k}_{H_2,ad}, K_H \qquad [6]$$

$$S{-}H \leftrightarrows S + H^+ + e^- \quad \vec{k}_{H,ox} \qquad [7]$$

The following mechanism is adapted for CO electro-oxidation:[27,29] CO molecules adsorb in a linear state, *i.e.*, one adsorption site per CO molecule

Table II. Model parameters used in simulation.

K_{CO}	2×10^{-7} atm[a]	$\vec{k}_{OH}$	8×10^{-4} A cm^{-2} [e]
K_H	0.5 atm[a]	$\overleftarrow{k}_{OH}$	2760 A cm^{-2} [b]
α_H	1/2	x^0_{CO}	108×10^{-6}
α_{CO}	1/2	T	315 K
α_{OH}	1/2	C_{dl}	0.45 F[c]
$\vec{k}_{H,ox}$	4.0 A cm^{-2} [a]	γ	100[d]
$\vec{k}_{H_2,ad}$	402 A cm^{-2} atm^{-1} [a,f]	C^*_t	2.2×10^{-9} mol/cm^2 [b]
$\vec{k}_{CO,ad}$	150 A cm^{-2} atm^{-1} [a,f]	A	5 cm^2
$\vec{k}_{CO,ox}$	5.5×10^{-4} A cm^{-2} [e]	p_{H_2}	2.96 atm
i	0.3 A/cm^2	v_0	48.1 sccm
V_A	2.63×10^{-7} m^3		

[a] Ref. 36.
[b] Ref. 37.
[c] Ref. 19.
[d] Estimated by the specific surface area of 20 wt % E-TEK PtRu/C catalyst and an electrochemical efficiency (utilization) of the anode catalyst of about 30%.
[e] Fitted parameters.
[f] Values increased by a factor of 10 from the original value in order to match the simulated oscillation frequency with the experimental results.

$$CO + S \leftrightarrows S{-}CO \quad \vec{k}_{CO,ad}, K_C \qquad [8]$$

This process is assumed to be reversible. Water is dissociated into surface hydroxyl group, OH

$$H_2O + S \leftrightarrows S{-}OH + H^+ + e^- \quad \vec{k}_{OH},\ \overleftarrow{k}_{OH} \qquad [9]$$

Finally, adsorbed CO reacts with the adsorbed hydroxyl group to form CO_2

$$S{-}OH + S{-}CO \rightarrow 2S + CO_2 + H^+ + e^- \quad \vec{k}_{CO,ox} \qquad [10]$$

This step is assumed to be irreversible.

Surface kinetics.—From Eq. 6, the net adsorption rate for H_2 is

$$r_{H_2,ad} = \vec{k}_{H_2,ad} p_{H_2} \theta_0^2 - \overleftarrow{k}_{H_2,ad} K_H \theta_H^2 \qquad [11]$$

where θ_0 is the fraction of free surface sites, which is from the total site balance

$$\theta_0 = 1 - \theta_{CO} - \theta_H - \theta_{OH} \qquad [12]$$

$\vec{k}_{H_2,ad}$ is the adsorption rate constant of H_2, and K_H is the equilibrium constant for H_2 desorption (the reciprocal of the adsorption equilibrium constant). θ_{CO}, θ_H, and θ_{OH}, are the surface coverages of CO, H, and OH, respectively. p_{H_2} is the partial pressure of hydrogen in the anode chamber.

The rate for hydrogen electro-oxidation, Reaction 7 is assumed to obey the Butler-Volmer equation

$$r_H = 2\vec{k}_{H,ox} \theta_H \sinh\left(\frac{\alpha_H F \eta_A}{RT}\right) \qquad [13]$$

where $\vec{k}_{H,ox}$ is the rate constant of H_2 electro-oxidation, α_H is the transfer coefficient, assumed to be the same for the forward and reverse reaction, and η_A is the anode overpotential. The other parameters have their usual meaning.

The net rate of CO adsorption is

$$r_{CO,ad} = \vec{k}_{CO,ad} x_{CO} p_{H_2} \theta_0 - \overleftarrow{k}_{CO,ad} K_C \theta_{CO} \qquad [14]$$

where $\vec{k}_{CO,ad}$ is the rate constant of CO adsorption, K_C is the equilibrium constant for CO desorption (the reciprocal of the adsorption equilibrium constant), and x_{CO} is the mole fraction of CO in the dry (water free) anode gas.

The water dissociative adsorption is an electrochemical step (Eq. 9) so that the rate depends upon the anode potential. This process is assumed to be reversible and to obey the Butler-Volmer equation, namely

$$r_{OH} = \vec{k}_{OH}\theta_0 \exp\left(\frac{\alpha_{OH}F\eta_A}{RT}\right) - \overleftarrow{k}_{OH}\theta_{OH} \exp\left(\frac{-(1-\alpha_{OH})F\eta_A}{RT}\right) \quad [15]$$

where $\vec{k}_{OH}$ and $\overleftarrow{k}_{OH}$ are the adsorption and desorption rate constants of water, and α_{OH} is the transfer coefficient for the reaction.

The CO oxidation step (Eq. 10) is considered as an irreversible electrochemical step with charge transfer. Thus

$$r_{CO} = \vec{k}_{CO,ox}\theta_{CO}\theta_{OH} \exp\left(\frac{\alpha_{CO}F\eta_A}{RT}\right) \quad [16]$$

where $\vec{k}_{CO,ox}$ is the rate constant of CO electro-oxidation, and α_{co} is the transfer coefficient for CO electro-oxidation.

Mass balance and charge conservation.—With these rate expressions, we can write the following unsteady-state site balance for the time evolution of the surface coverage of CO, H, and OH

$$(F\gamma C_t^*)\frac{d\theta_{CO}}{dt} = r_{CO,ad} - r_{CO} \quad [17]$$

$$(F\gamma C_t^*)\frac{d\theta_H}{dt} = r_{H_2,ad} - r_H \quad [18]$$

$$(F\gamma C_t^*)\frac{d\theta_{OH}}{dt} = r_{OH} - r_{CO} \quad [19]$$

where γ is the roughness factor of the electrode (in the units of cm^2 PtRu/cm^2 electrode), and C_t^* is the atom mole density per cm^2 PtRu surface.

The material balance for species i in the anode chamber is

$$V_A\frac{dc_i}{dt} = v_0c_{i,0} - vc_i - N_iA \quad [20]$$

where V_A is the volume of the electrode chamber, assumed here to be well mixed. v_0 and v are the volumetric inlet and outlet anode flow rates, respectively, $c_{i,0}$ and c_i are the concentrations of species i in the inlet and outlet streams, respectively, N_i is the flux of species i into the MEA, and A is the geometric area of the MEA in the fuel cell. The flux N_i of H_2, CO, or any other species is, in principle, affected by mass-transfer limitations through the gas diffusion layer and catalyst layer, as well as by the kinetics of the electrode reactions,[25] but it is reasonable here to assume that the fluxes of CO as well as H_2 are determined solely by the anode kinetics, the limiting current densities being considerably higher than the current densities utilized in this study.

Applying Eq. 20 for the case of CO results in Eq. 21, which governs the time variation of the CO concentration in the anode chamber

$$\frac{p_{H_2}V_A}{RT}\frac{dx_{CO}}{dt} = \frac{P_0v_0}{RT_0}x_{CO}^0 - \frac{P_0v}{RT_0}x_{CO} - \frac{A}{F}r_{CO,ad} \quad [21]$$

where T is the fuel-cell temperature, V_A is the volume of the anode chamber, and x_{CO}^0 and x_{CO} are the CO mole fractions in the anode feed and the anode compartment outlet, respectively. Note that the volumetric flow rates are measured at 1 atm and 298 K, so that P_0 is 1 atm and T_0 is 298 K, and not the fuel-cell operating pressure and temperature.

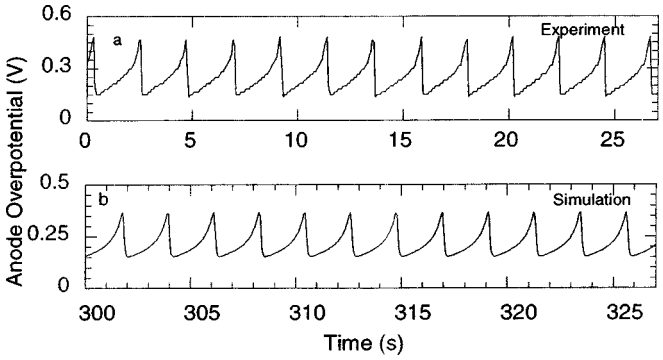

Figure 11. Comparison between experimental and simulation results. Fuel-cell temperature 42°C; current density 300 mA/cm^2; anode inlet flow rate 48.1 sccm. Parameter values used are listed in Table II.

Similarly, Eq. 20 as applied to H_2 in the anode chamber provides

$$\frac{P_0v}{RT_0} = \frac{P_0v_0}{RT_0} - \frac{A}{2F}r_{H_2,ad} \quad [22]$$

Considering capacitive and faradaic currents and using the equation of charge conservation, the equation for the time evolution of the electrode potential is obtained. The total current is the sum of the faradaic current and the capacitive current (double-layer charging and discharging current). The capacitive current is written as the product of the double-layer capacity C_{dl} and the temporal change of the potential. The faradaic current includes H and CO electro-oxidation current and the net current of water dissociation

$$C_{dl}\frac{d\eta_A}{dt} = A(i - r_H - r_{CO} - r_{OH}) \quad [23]$$

The resulting system of coupled ordinary differential equations ODEs (Eq. 17-19, 21, 23) were solved with Berkeley-Madonna software (Kagi Shareware, Berkeley, CA) using a fourth-order Runge-Kutta routine. The parameters used in the simulation are listed in Table II.

Simulation results.—The simulation results are shown in Fig. 11, together with experimental results under the same conditions, while a magnified simulation result is shown in Fig. 8b to contrast with the experimental data. It is clear that the simulated oscillation curve captures all of the essential features of the anode potential oscillations. The simulation predicts that the anode overpotential increases gradually to a high value and then drops to a lower value rapidly, as experimentally observed. The predicted oscillation frequency and the amplitude are also very close to the experimental value. The period is about 2.5 s, which is the same as in experiments. The simulated potential oscillation range is 0.14-0.38 V, with the maximum overpotential some 0.07 V lower than the corresponding experimental value. This good agreement between experimental and simulation results supports the qualitative interpretation of this oscillatory phenomenon described earlier in this paper.

The computed time evolution of five system variables is shown in Fig. 12. It is seen, as expected, that the surface coverages of CO, H, and OH oscillate together with the resulting periodic oscillation of CO mole fraction in the anode chamber and the anode overpotential. It may be noted that although the three surface species coverages oscillate simultaneously, the catalyst surface is dominated by CO. The gas-phase CO concentration is also predicted to oscillate within a narrow range at the experimental conditions used. It is also

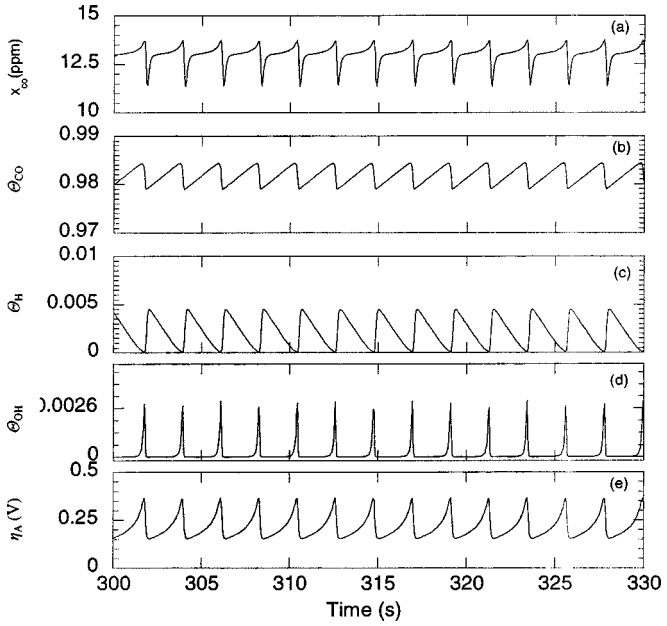

Figure 12. Time evolution of (a) anode CO mole fraction, (b) surface coverage of CO, (c) surface coverage of H, (d) surface coverage of OH, and (e) anode overpotential for conditions of Fig. 11. Parameter values used are listed in Table II.

interesting to note that these different variables assume different shapes in the time evolution. Figure 13 shows the locus of the limit cycle for some of the variables in phase diagram.

It is found in the simulation that the electro-oxidation rate constant of CO, $\vec{k}_{CO,ox}$, is a key and a very sensitive parameter for the oscillations to appear. The oscillation patterns simulated with different values of the rate constant are shown in Fig. 14. It is seen from the figure that with the increase of the rate constant, the oscillation frequency becomes larger and eventually, the oscillations extinguish at still larger values. This result looks qualitatively similar to the temperature effect on oscillation (Fig. 7). The increase of the rate constant may be viewed as a result of the increase of fuel-cell temperature. A rigorous simulation of the temperature effect requires the introduction of appropriate activation energies for the rate constants. Further, a detailed bifurcation analysis is needed to understand the parameter dependence of the oscillatory phenomenon. This part of the work is now underway.

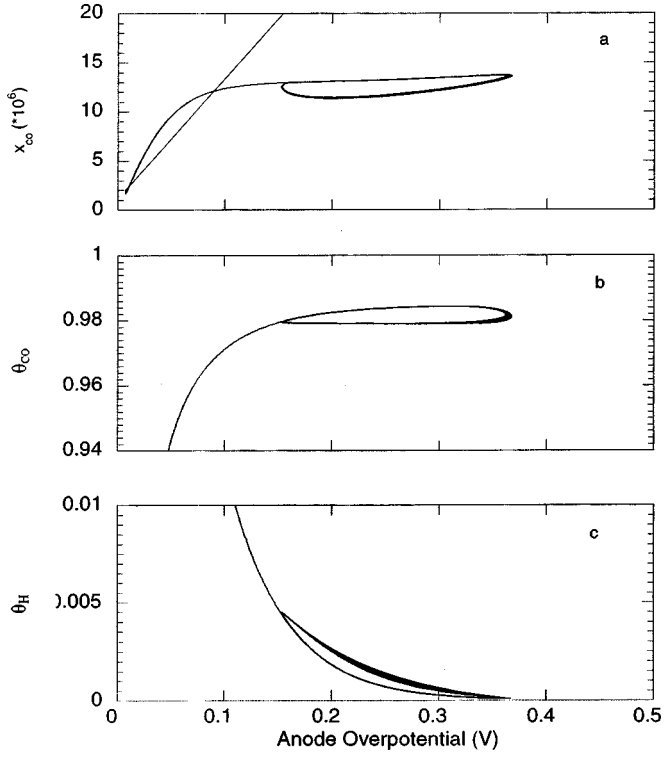

Figure 13. Computed phase diagram: (a) anode CO mole fraction, (b) surface coverage of CO, and (c) surface coverage of H *vs.* anode overpotential.

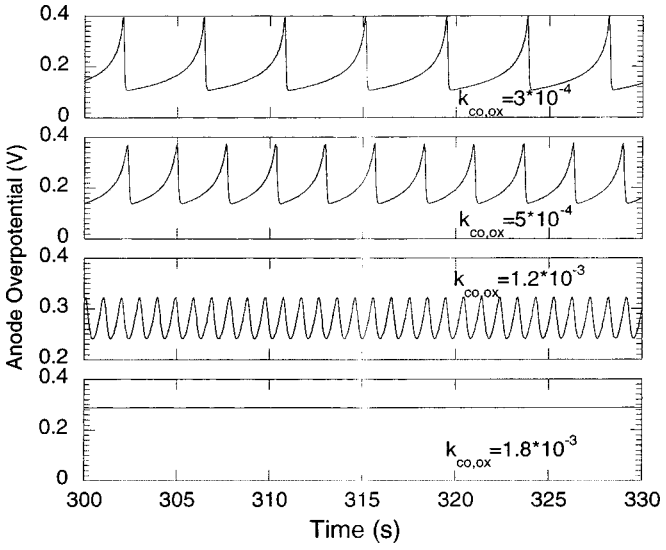

Figure 14. Simulated potential oscillation patterns with different values of the CO electro-oxidation rate constant. All other parameter values are the same as in Table II.

In short, with this realistic but simple model, we have shown mechanistically and mathematically that the potential oscillations can exist with a H_2/CO feed to a PEM fuel-cell anode. The agreement between experimental and simulation results lends credence to our explanation of the anode kinetics of H_2/CO electro-oxidation on PtRu catalyst. This model can also be applied to predict the steady-state performance of PtRu anode catalyst with CO impurities in anode feed. Further, it indicates that the parameter values used in this simulation are reasonable but need to be further investigated.

Conclusions

Sustained potential oscillations are found experimentally in a PEM fuel cell operating at constant current density with PtRu as anode catalyst and a H_2/108 ppm CO as anode feed gas. The potential oscillations appear at certain operating conditions determined by fuel-cell temperature, current density, and anode flow rate. A preliminary qualitative analysis indicates that these potential oscillations are due to the coupling of the electro-oxidation of H_2 and CO on the binary PtRu alloy surface. Ru may be acting as the key component in the formation of OH_{ad} from water, which is the oxidation agent of CO_{ad}. The qualitative analysis also shows that a surface process may be controlling the potential oscillations, such as the dissociation of H_2O or the electro-oxidation of CO. A simple but realistic kinetic model is proposed which reproduces the observed oscillatory phenomenon. The rate constant of CO oxidation is found to be a key parameter in the onset of oscillations.

Acknowledgment

We thank Dr. Ilie Fishtik and Dr. Faisal Syed for their help with LabVIEW and Berkeley-Madonna software. J.Z. also gratefully acknowledges the Dr. Chue-san Yoo Fellowship for partial support of his graduate study.

Worcester Polytechnic Institute assisted in meeting the publication costs of this article.

References

1. T. R. Ralph, *Platinum Met. Rev.*, **41**, 102 (1997).
2. B. E. Conway and D. M. Novak, *J. Phys. Chem.*, **81**, 1459 (1977).
3. P. Russell and J. Newman, *J. Electrochem. Soc.*, **133**, 59 (1986).
4. P. Russell and J. Newman, *J. Electrochem. Soc.*, **134**, 1051 (1987).
5. J. St-Pierre and D. L. Piron, *J. Electrochem. Soc.*, **137**, 2491 (1990).
6. D. L. Piron, I. Nagatsugawa, and C. Fan, *J. Electrochem. Soc.*, **138**, 3296 (1991).
7. H. Okamoto, N. Tanaka, and M. Naito, *J. Electrochem. Soc.*, **147**, 2629 (2000).
8. H. Okamoto, N. Tanaka, and M. Naito, *J. Phys. Chem. A*, **102**, 7353 (1998).
9. H. Okamoto, N. Tanaka, and M. Naito, *J. Phys. Chem. A*, **102**, 7343 (1998).
10. G. Inzelt and V. Kertesz, *Electrochim. Acta*, **40**, 221 (1995).
11. G. Inzelt and V. Kertesz, *Electrochim. Acta*, **42**, 229 (1997).
12. V. Kertesz, G. Inzelt, C. Barbero, R. Kotz, and O. Haas, *J. Electroanal. Chem.*, **392**, 91 (1995).
13. H. Hunger, *J. Electrochem. Soc.*, **115**, 492 (1968).
14. G. Horanyi and C. Visy, *J. Electroanal. Chem.*, **103**, 353 (1979).
15. T. Yamazaki, T. Kodera, R. Ohnishi, and M. Masuda, *Electrochim. Acta*, **35**, 431 (1990).
16. K. Krischer, M. Lubke, W. Wolf, M. Eiswirth, and G. Ertl, *Ber. Bunsenges. Phys. Chem.*, **95**, 820 (1991).
17. T. Yamazaki and T. Kodera, *Electrochim. Acta*, **36**, 639 (1991).
18. S. Szpak, *J. Electrochem. Soc.*, **117**, 1056 (1970).
19. M. C. Deibert and D. L. Williams, *J. Electrochem. Soc.*, **116**, 1291 (1969).
20. W. Wolf, K. Krischer, M. Lubke, M. Eiswirth, and G. Ertl, *J. Electroanal. Chem.*, **385**, 85 (1995).
21. H. Okamoto, N. Tanaka, and M. Naito, *Chem. Phys. Lett.*, **248**, 289 (1996).
22. P. Strasser, M. Eiswirth, and G. Ertl, *J. Chem. Phys.*, **107**, 991 (1997).
23. M. Murthy, M. Esayian, A. Hobson, S. MacKenzie, W. Lee, and J. W. Van Zee, *J. Electrochem. Soc.*, **148**, A1141 (2001).
24. G. Ertl, *Science*, **254**, 1750 (1991).
25. T. Thampan, S. Malhotra, J. Zhang, and R. Datta, *Catal. Today*, **67**, 15 (2001).
26. J. Zhang, T. Thampan, and R. Datta, *J. Electrochem. Soc.*, **149**, A765 (2002).
27. H. A. Gasteiger, N. M. Markovic, and P. N. Ross, *J. Phys. Chem.*, **99**, 8290 (1995).
28. T. J. Schmidt, H. A. Gasteiger, and R. J. Behm, *J. Electrochem. Soc.*, **146**, 1296 (1999).
29. H. A. Gasteiger, N. M. Markovic, and P. N. Ross, *J. Phys. Chem.*, **99**, 16757 (1995).
30. J. W. Bauman, T. A. Zawodzinski, Jr., and S. Gottesfeld, in *Proton Conducting Membrane Fuel Cells II*, S. Gottesfeld and T. F. Fuller, Editors, PV 98-27, p. 136, The Electrochemical Society Proceedings Series, Pennington, NJ (1997).
31. A. V. Zeigarnik, R. E. Valdes-Perez, and J. Pesenti, *J. Phys. Chem. B*, **104**, 997 (2000).
32. E. Shustorovich and H. Sellers, *Surf. Sci. Rep.*, **31**, 1 (1998).
33. N. M. Markovic, T. J. Schmidt, B. N. Grgur, H. A. Gasteiger, R. J. Behm, and P. N. Ross, *J. Phys. Chem. B*, **103**, 8568 (1999).
34. A. B. Anton and D. C. Cadogan, *Surf. Sci.*, **239**, L548 (1990).
35. J. B. Day, P. Vuissoz, E. Oldfield, A. Weichowski, and J. Ansermet, *J. Am. Chem. Soc.*, **118**, 13046 (1996).
36. T. E. Springer, T. Rockward, T. A. Zawodzinski, and S. Gottesfeld, *J. Electrochem. Soc.*, **148**, A11 (2001).
37. M. T. Koper, T. J. Schmidt, N. M. Markovic, and P. N. Ross, *J. Phys. Chem. B*, **105**, 8381 (2001).